

EVOLUTIONARY EMERGENCE OF NEURODYNAMIC NETWORKS FOR ROBUST CONTROL: A SIMPLE EXCITATORY-INHIBITORY NETWORK

006 **Anonymous authors**

007 Paper under double-blind review

ABSTRACT

013 Fine-grained network models based on differential equations, and neurodynamic
 014 synapses and neurons provide a realistic description of biological neuronal net-
 015 works, compared with mainstream artificial neural networks. They nevertheless
 016 have not been widely explored, mainly due to the lack of effective parameter train-
 017 ing methods. We propose a neurodynamic model training method that combines
 018 an efficient neurodynamic simulation architecture and an evolutionary algorithm.
 019 Based on a simple Excitatory-Inhibitory network, a neurodynamic model with task
 020 control capabilities is successfully obtained via parallel dynamic simulation, and
 021 network selection methods under evolutionary pressure. Compared with the state-
 022 of-the-art reinforcement learning methods, the resulting neurodynamic network
 023 can achieve comparable task control performance for Mujoco tasks in a signifi-
 024 cantly smaller network scale within fewer training steps. Our work provides an
 025 alternative path to functional networks alongside mainstream reinforcement learn-
 026 ing frameworks, and prove the feasibility of the evolutionary approach toward
 027 biological intelligence.

1 INTRODUCTION

030 Living organisms in nature can rapidly adapt to the complex environment while interacting with it in
 031 the absence of explicit supervision conditions under evolutionary pressure, where the neural systems
 032 play an important role in continuous evolution and adaptation to the environment. Early efforts on
 033 modelling biological neural networks focused extensively on the dynamics of neuronal electrophys-
 034 iological activities, Hodgkin & Huxley (1952) aiming to simulate biological mechanisms. However,
 035 due to the limitations on computational resources at the time, the large-scale applications of bio-
 036 inspired dynamic models were challenging. Therefore more simplified artificial neural network
 037 (ANN) was proposed, McCulloch & Pitts (1943) and has been extensively used up to date. With the
 038 introduction of backpropagation algorithms, ANNs have proved their capabilities in several appli-
 039 cation scenario. LeCun et al. (2015) ANNs rely on the training using large-scale labelled data, with
 040 the static input-output mapping as the main processing method, Zador (2019) which abandons the
 041 rich temporal dynamics in biological neural systems. Conventional ANNs have not only succeeded
 042 in supervised learning tasks, their applications in reinforcement learning have also been widely ex-
 043 plored, especially in scenarios where intelligences need to continuously optimise their strategies
 044 while interacting with the external environment. In fact, the central idea of reinforcement learning
 045 is essentially derived from the abstraction of the adaptive behaviour of living organisms: instead
 046 of relying on large-scale labelled samples, living organisms develop effective interacting strategies
 047 through continuous interaction with the environment, and shape by natural selection. This capability
 048 allows living organisms to process certain structures *a priori*, and learning rules, and thus to rapidly
 049 develop functional models under limited resources.

050 The modelling on the dynamics of neural systems has increasingly drawn attention in recent years.
 051 Van and Sompolinsky proposed the excitation-inhibition balance network, Vreeswijk & Sompolin-
 052 sky (1996) which possesses rich dynamical features, Brunel (2000) and explains the experimentally
 053 observed irregular network firing under constant external input. Subsequent studies employed the
 054 excitation-inhibition balance as a basic principle to construct computational models for different
 055 functional areas of the human brain, including visual cortex Potjans & Diesmann (2014); Schmidt

054 et al. (2018), motor cortex Hennequin et al. (2014) and decision-making cortex Wong & Wang
 055 (2006). Later, the spiking neural network (SNN) Maass (1997) and continuous-time neurodynamic
 056 models were proposed to model the biological neural activity. The effective training of neurody-
 057 namic models, however, still faces several challenges, since they are normally highly non-linear
 058 with complex gradient propagation paths, and models driven by pulse events, *e.g.*, SNNs, are inher-
 059 ently non-differentiable, making the direct applications of backpropagation algorithms impossible.
 060 Several studies have attempted to introduce surrogate gradient, Neftci et al. (2019) or local learn-
 061 ing rules Markram et al. (2012) to improve the trainability, however, these approaches still have
 062 significant gaps in terms of convergence speed, stability, and task adaptability, compared with the
 063 mainstream deep learning frameworks. Therefore, the development of new training paradigms suit-
 064 able for neurodynamic models remains a key path to bring artificial systems closer to biological
 065 intelligence.

066 Evolutionary algorithm (EA) Sampson (1976) is inspired from the biological evolution mechanism,
 067 and has been applied to neural network training and strategy optimisation. EA does not rely on
 068 backpropagation or exact gradient information, enabling neural networks to gradually evolve func-
 069 tionally stable networks in complex time-varying environments. Its application on the training of
 070 neural dynamical systems, however, still remains difficult. Dynamic systems are temporally highly
 071 coupled, and the state evolution process relies on continuous numerical integration, or impulse-
 072 driven updating, requiring significantly higher computational overheads than static feed-forward
 073 networks. Therefore traditional evolutionary algorithms are normally unable to meet the training
 074 requirements in terms of efficiency and scalability, and the effective applications of evolutionary
 075 algorithm optimisation in dynamic models have long been limited by computational resources.

076 Evolutionary optimisation of biologically inspired networks has been explored in several recent stud-
 077 ies. Shen et al. (2023) evolved spiking microcircuits for control tasks, demonstrating the feasibility
 078 of structural evolution in SNNs. Habashy et al. (2024) analysed how heterogeneous neuronal time
 079 constants shape functional dynamics, suggesting the importance of biophysical diversity. Najarro &
 080 Risi (2020) employed evolution to meta-optimise Hebbian plasticity rules for deep networks, high-
 081 lighting an alternative route toward biologically motivated learning. Our work differs from these
 082 approaches by jointly optimising synaptic delays and weights at scale, enforcing E-I balanced pop-
 083 ulation structure, and integrating these components into a unified neurodynamic model evaluated on
 084 continuous-control tasks.

085 In the current study, we modify the evolutionary algorithm optimisation on neurodynamic systems,
 086 and propose a novel evolutionary training paradigm for neurodynamic models. The adaptation of
 087 individuals while interacting with the environment is simulated by evolving a dynamic model over
 088 time in a reinforcement learning environment, and the evolution of a population of individuals is
 089 simulated by a parallelised evolutionary algorithm, following a bio-inspired optimisation strategy.
 090 We introduce a high-performance dynamical simulation framework ENLARGE, Qu et al. (2023)
 091 which is based on a fine-grained network representation and hierarchical communication architec-
 092 ture, and redesign the data structure of neuron and synapse model to preserve the biological features
 093 of the network. We also compare two efficient fitness assessment strategy, the Covariance Matrix
 094 Adaptation Evolution Strategy (CMA-ES) Hansen et al. (2003) and the Natural Evolution Strategy
 095 (NES), Wierstra et al. (2014) and parallelise the network parameter optimisation in the evolutionary
 096 algorithm to further enhance its efficiency. Our model starts from an initial network with excitatory
 097 and inhibitory (E-I) neurons, and gradually evolves a functional network with control capability.

098 **Contributions** The contributions of this paper can be summarised as follows:

- 099 • Different from the existing ANN and SNN models, we propose a novel biological neuro-
 100 dynamic network (BNN) model to describe intelligent behavior.
- 101 • Integrating efficient dynamical simulation with parallel evolutionary algorithms accelerates
 102 BNN training and improves sampling efficiency in reinforcement learning.
- 103 • The BNN achieves comparable performance across MuJoCo tasks with significantly fewer
 104 training steps and a much smaller network size.

105 The aim of our study is not to surpass state-of-the-art performance in any given reinforcement learn-
 106 ing task. Instead, we present a new modelling and training framework that provides a parallel path
 107 to existing mainstream reinforcement learning frameworks from a self-organisation perspective. As

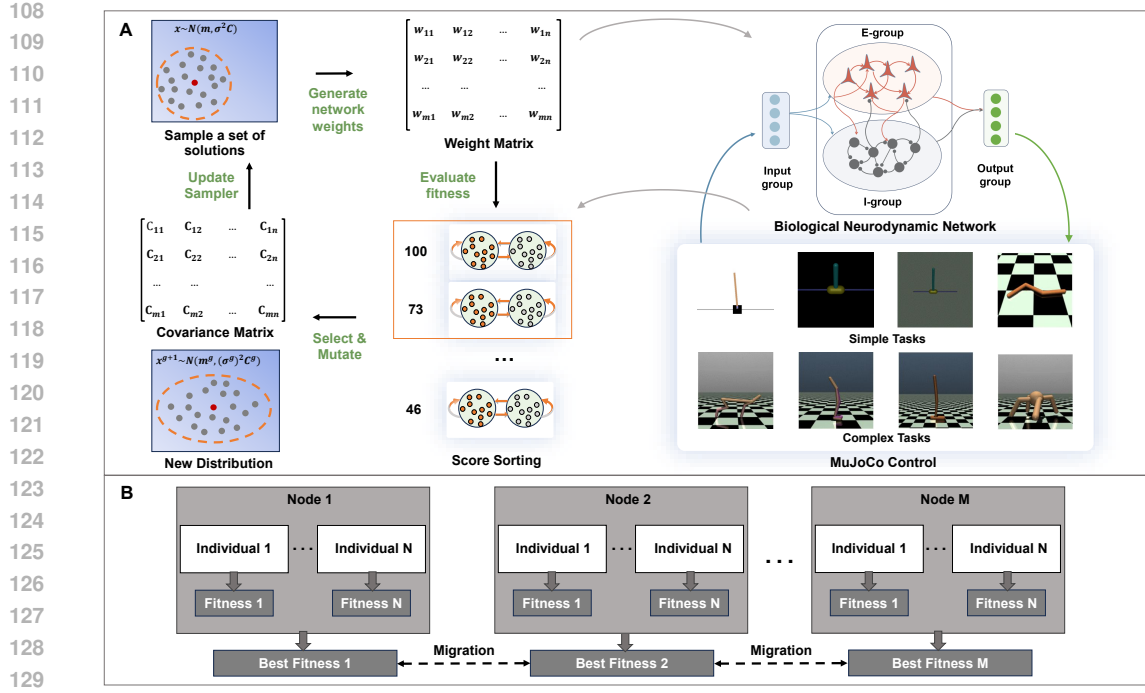


Figure 1: Illustration of the training paradigm.(A) The flowchart of the Biological Neurodynamic Network (BNN) optimisation. The model is optimised using the evolutionary algorithm starts by sampling a set of solutions to generate the parameter matrix. The fitness of the dynamics network is then evaluated through the interaction of reinforcement learning with Mujoco tasks of different difficulties. The parameters of the the distribution are updated using selection and variation operators as the next generation in the evolutionary algorithm. (B) Parallel accelerated framework. M nodes are set up in the cluster, and N tasks are assigned to each node according to the population size. The optimal fitness is computed for each node in each generation. The optimal parameters of the population are exchanged at a fixed interval, *i.e.*, Migration.

a proof-of-principle study, we successfully achieved the evolution of the neurodynamic model in a real reinforcement learning environment, thus providing an alternative path for building interpretable and evolvable brain-like intelligent systems.

2 RELATED WORKS

Neurodynamic Models Since the pioneer works by Hodgkin and Huxley, Hodgkin & Huxley (1952) the concept of neurodynamics has been raised and studied extensively. Most studies employ a set of differential equations that describes the propagation of empirical action potential data, and the model size is normally limited to few neurons. Most neurodynamic models focused on the dynamic features, and little has been attempted to account for the behaviour. Artificial neural networks were proposed with similar origins. McCulloch & Pitts (1943) However, they quickly focused on describing the behaviour; artificial neural networks have thus diverged from neurodynamic models. Newell et al. (1958); Rosenblatt (1958) The limited understanding of the neural basis of behaviour at the time left artificial intelligence and machine learning largely disconnected from neuroscience. With the development of neuroscience and the modern computation industry, attempts have been made to propose more biologically realistic models, where a central focus is the dynamic features, which have mostly been ignored by artificial neural networks. A number of neurodynamic models Eliasmith & Anderson (2003) have been proposed, which provide an alternative path to describe intelligent behaviour.

162

163 Table 1: A comparison of the performances of different optimisation algorithms on Mujoco tasks
164 reported in the literature. Schulman et al. (2017); Salimans et al. (2017b)

Optimisation Approach	Gradient-based (PPO)	Evolution Strategies
Environment Step(s)	10^6	10^7
Benchmark Model/Size	MLP/(64,64)	MLP/(64,64)
Rewards		
HalfCheetah	~ 2000	~ 4500
Hopper	~ 2200	~ 2100
InvertedDoublePendulum	~ 8000	~ 7000
InvertedPendulum	1000	1000
Swimmer	~ 120	~ 121
Walker2d	~ 2500	~ 2500

175

176

177 **Gradient-based optimisation methods** have been widely used in deep reinforcement learning
178 (DRL) in recent years, driving rapid development from gaming intelligences, *e.g.*, Atari, Go, to
179 robotic control systems. Deep Q-Network (DQN) Mnih et al. (2015) was the first to combine
180 convolutional neural networks and Q-learning to achieve end-to-end effective learning strategies from
181 high-dimensional pixel inputs. Subsequently, algorithms such as Trust Region Policy Optimization
182 (TRPO), Schulman et al. (2015) and Proximal Policy Optimization (PPO) Schulman et al. (2017)
183 have improved deep learning in terms of convergence efficiency and policy stability, and become the
184 current mainstream policy optimisation method. However, the success of such frameworks relies
185 heavily on highly engineered network structures and training techniques, with limited interpretability.
186 When confronted with more biologically realistic neural systems, these methods face difficulties
187 such as instability, difficult or unfeasible gradient computation, and the likelihood of being trapped
188 at local optima, thus severely limiting the trainability and convergence of the model.

189

190 **Evolutionary algorithm** (EA), as a population-based, gradient-free evolutionary optimisation strategy,
191 it provides a robust and scalable alternative for network parameter optimisation. It has been
192 shown that employing evolutionary algorithms to train policy networks can achieve performance
193 comparable to mainstream gradient-based algorithms in reinforcement learning tasks. Such et al.
194 (2018) Furthermore, structural evolution methods such as HyperNEAT Stanley et al. (2009) demon-
195 strate the advantages of evolutionary algorithms in terms of structural interpretability and modularity
196 generation. Stanley & Miikkulainen (2002) EAs have unique advantages in the optimisation of neu-
197 rodynamic models as they do not rely on gradient information. Few works have attempted to apply
198 evolutionary algorithms to neurodynamic network training, Mozafari et al. (2019) they nevertheless
199 are still unable to present a systematic solution. A comparison of the performance of optimisation
200 methods is presented in table 1. Both optimisation algorithms can achieve excellent performances
201 on MuJoCo tasks, but they require a complex network consisting of hundreds of neurons, and mil-
202 lions of optimisation steps. For comparison, the main model described in this paper contains only
203 20 neurons, and can achieve comparable results using an evolutionary algorithm trained for 5×10^5
204 steps.

205

206

3 PRELIMINARIES

207

208

209 **E-I balance** Neurons and synapses in the brain coordinate their excitatory and inhibitory inputs
210 to establish and maintain a constant excitation-inhibition (E-I) ratio, which is known as E-I balance.
211 Shadlen & Newsome (1994) The excitation-inhibition balance is one of the fundamental properties
212 of the cerebral cortex, and it has been shown that this balance is prevalent in a wide range of cortical
213 areas. Isaacson & Scanziani (2011); Haider & McCormick (2009) E-I balance also benefits the pre-
214 cision and efficiency of neuronal coding mechanisms, Denève & Machens (2016) extensive dynamic
215 simulations further reveal that the E-I balanced structure is capable of generating rich computational
216 dynamic behaviours, Vreeswijk & Sompolinsky (1996); Brunel (2000); Denève et al. (2017) and
217 thus acts as potential building blocks of brain functions. Furthermore, recent studies suggest that
218 training an E-I balanced network as the initial state can significantly improve the learning efficiency
219 and stability of the network. Song et al. (2016); Ingrossi & Abbott (2019)

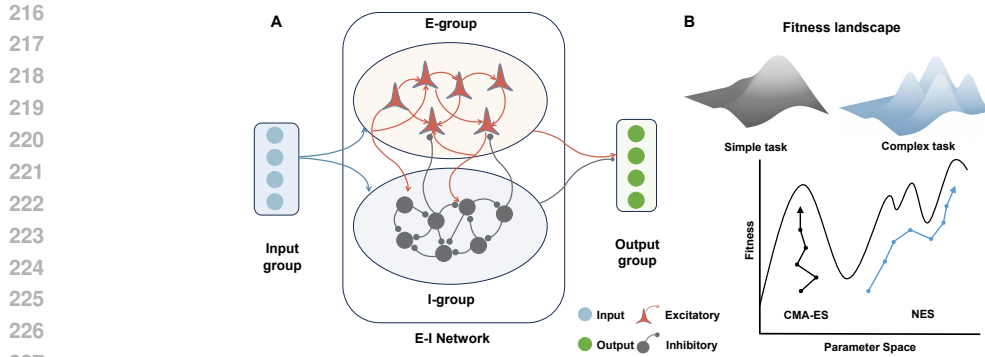


Figure 2: Illustration of the BNN architecture, and Evolutionary Algorithms. (A) Neurons are grouped into four types: input, excitatory (E), inhibitory (I), and output, coloured in blue, red, gray and green, respectively. Connections are established between neurons in all groups via two types of synapses: excitatory and inhibitory, coloured in red and gray, respectively. (B) Illustration of two evolutionary algorithms. CMA-ES is more efficient on optimisation on simple energy landscapes, whereas NES is fundamentally more suitable for multifunnel landscapes.

Beyond biological plausibility, balanced E-I networks also offer concrete functional advantages in machine learning contexts. Prior theoretical and computational studies (Wang (1999); Brunel (2000)) demonstrate that E-I balance stabilises network dynamics, speeds convergence toward attractor states, and increases robustness to noisy inputs. More recent work shows that initializing networks in an E-I balanced regime can substantially reduce the number of training steps needed to reach competent performance by constraining neural activity within dynamically stable regions of state space. These considerations motivate the inclusion of E-I balance in our evolutionary framework.

Spiking Neural Networks As the most widely used model in computational neuroscience and neuromorphic computing, the Spiking Neural Network (SNN) Maass (1997); Maass & Markram (2004) provides a realistic whilst computationally feasible description of biological neural networks, compared with traditional neural networks. In a SNN, neurons are connected with each other arbitrarily via synapses, and the states of neurons and synapses are updated in cycles by firing a large number of spikes as signals. The biologically relevant features of SNN, Winer (1993) however, make the direct application of SNNs in high performance computation difficult. Many computational frameworks have been proposed to address the efficiency problem, *e.g.*, NEST, Gewaltig & Diesmann (2007) GeNN, Yavuz et al. (2016) and ENLARGE. Qu et al. (2023) In the current work, we modify the traditional SNN in the ENLARGE framework, such that continuous postsynaptic currents instead of discrete spikes are transmitted across the networks of neurons and synapses.

4 METHODS

4.1 BIOLOGICAL NEURODYNAMIC NETWORK

Our biological neardynamic network (BNN) is based on an Excitatory-Inhibitory network, Vreeswijk & Sompolinsky (1996) consisting of the Leaky Integrate-and-Fire (LIF) neuron model and AMPA/GABA synapses, Gerstner et al. (2014) with some modifications for better biological interoperability and viability.

Model for neuron Neurodynamic models require neuron models to describe the dynamics of neurons, *i.e.*, signal firing. Multiple models for neurons have been proposed; among them, the Leaky Integrate-and-Fire (LIF) neuron has been proved to be a biologically realistic and computationally feasible one. The majority of SNNs are established by deterministic neurons, whereas biological neurons have inherent randomness in terms of firing. Ma et al. (2023) We introduce a novel **noisy input current term** into LIF neurons as an analogue to the random disturbances of real biological neurons.

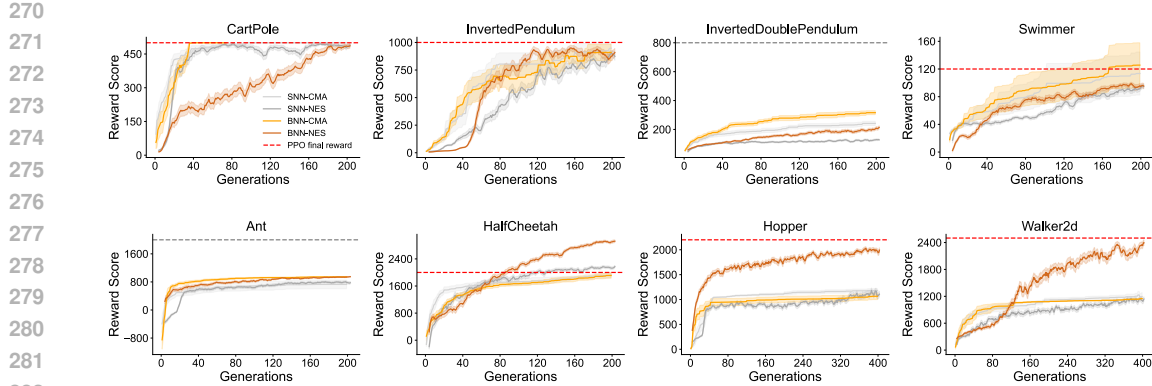


Figure 3: Performance of biological neurodynamic netwrok (BNN) and SNN on MuJoCo tasks. The dashed line indicates the state-of-the-art reference reward value achieved by PPO method reported in literature. Schulman et al. (2017)

Model for synapse In addition to neurons, the connections between them, *i.e.*, synapses, are crucial in biological neural networks. Synapses transmit electrical signals from presynaptic to postsynaptic neurons, it defines how signals fired by neurons affect the membrane voltage of a postsynaptic neuron. In the current work we choose to model two classes of synapses, AMPA and GABA, to describe the excitatory and inhibitory responses, respectively.

Synaptic connection strength, *i.e.*, synaptic weight, is the only trainable parameter in traditional neurodynamic models. Whereas in the real biological neural systems, the temporal order of signals from multiple synapses reaching the postsynaptic neuron is crucial to information encoding, hence this information processing fashion relies on synaptic delay. Mészáros et al. (2024) Therefore, we introduce **synaptic delay** as a novel parameter for better biological interoperability, which significantly improves the learning ability of our neurodynamic network.

Neurodynamic network Our network consists of 10 excitatory and 10 inhibitory neurons, and the number of neurons in the input and output group is dynamically adjusted according to the dimensionality of the task. Connections are established between all four groups within the network: Input, Excitatory (E), Inhibitory (I) and Output groups, via synapses. All the synapses starting from neurons in the Input, Output and E groups are excitatory, and synapses starting from the I group are inhibitory, as illustrated in figure 2A. This design follows Dale’s Law and is consistent with the suggestions outlined in Burns (2021), who argues that incorporating heterogeneous neuron classes and biophysical constraints can enhance adaptability and interpretability in reinforcement learning models. Our model operationalizes these principles within an evolutionary-optimisation framework rather than Hebbian learning.

4.2 SIMULATION FRAMEWORK

Evolutionary Algorithm We introduce two popular evolutionary algorithms, CMA-ES Hansen et al. (2003) and NES. Wierstra et al. (2014) Among them, CMA-ES adaptively adjusts the mean and variance of the sampling distribution by calculating the covariance matrix, and NES updates the distribution by calculating the gradient through the Riemannian metric. For simple tasks CMA-ES can quickly find the convex regions on single-funnel energy landscapes characterised by low-dimensional spaces, whereas NES, through natural gradient climbing, does not rely on local second-order structures, and is therefore suitable for non-convex, multi-funnel complex landscapes, as illustrated in figure 2B.

A distributed setup for EAs is employed in the current work, which uses the island model as the base model. It is able to effectively balance the population diversity and global search capability, and is suitable for parallelisation in a distributed computing environment (DEC). By defining independent sub-populations and a periodic migration mechanism, it is able to execute in parallel on multiple

324 computing nodes. The introduction of the migration mechanism promotes the global search, and
 325 reduces the possibility of being trapped at local optima.
 326

327 This design, inspired by population genetics, maintains partially isolated subpopulations that pro-
 328 mote behavioural diversity and prevent premature convergence. Prior work (e.g., Salimans et al.
 329 (2017a)) did not rely on such mechanisms due to massive compute budgets, but recent studies high-
 330 light that under limited compute and highly non-convex fitness surfaces, island structures stabilise
 331 training by preserving exploration across disconnected regions of the landscape. We therefore in-
 332 clude this mechanism to improve robustness of BNN optimisation.
 333

334 **Dynamic simulation framework** The parallel neurodynamics training framework ENLARGE Qu
 335 et al. (2023) is employed. We mainly use the fine-grained network representation and hierarchical
 336 communication architecture in ENLARGE.
 337

338 Unlike prior neuroevolution approaches such as Najarro Risi (2020), which optimize Hebbian plas-
 339 ticity rules within deep neural networks, our work directly evolves all parameters of a biologically
 340 grounded neurodynamic circuit—including synaptic delays, excitatory/inhibitory identity, and in-
 341 trinsic dynamics. This shifts the optimisation target from plasticity parameters in ANNs to the full
 342 parameterization of a biophysically interpretable dynamical system.
 343

344 5 EXPERIMENTS

345 We evaluate the above-described biological neurodynamic model, evolutionary algorithms and com-
 346 putational framework, and test them on multiple tasks from the MuJoCo environments. Todorov
 347 et al. (2012)

348 **Reinforcement learning task** Our BNN is assessed on a range of standard control tasks in a re-
 349 inforcement learning environment, OpenAI Gym, Brockman et al. (2016) including some simple
 350 control task such as Cartpole, InvertedPendulum, InvertedDoublePendulum, and Swimmer, as well
 351 as several high-dimensional continuous control tasks from the MuJoCo environment, Todorov et al.
 352 (2012) including Ant, HalfCheetah, Hopper, and Walker2d. These tasks involve robotic locomo-
 353 tion control characterised by high-dimensional state spaces (ranging from 4 to 27 dimensions) and
 354 continuous action spaces (1 to 8 dimensions).
 355

356 **Benchmark method** As benchmark algorithms, we used the Proximal Policy Optimization (PPO)
 357 Schulman et al. (2017) and the Trust Region Policy Optimization (TRPO) Schulman et al. (2015)
 358 implementation in RL-Baselines3-Zoo. Similarly, all tasks are implemented using the simulation
 359 environment provided by OpenAI Gym. Brockman et al. (2016) Both the policy and value functions
 360 are modelled as fully connected multi-layer perceptrons (MLPs) with two hidden layers of 64 units
 361 each, within tanh activations. Each task is trained for 5×10^5 steps, and performance is evaluated as
 362 the average return over 10 runs with different random seeds.
 363

364 **Network parameter training** We employ the CMA-ES and NES fitness assessment strategy in
 365 the ENLARGE framework. λ weights are sampled from a $[0, 1]$ random distribution as the initial
 366 individuals; then the fitness levels are assessed for individuals, and return to the main evolutionary
 367 algorithm; μ individuals with highest fitness values are selected to update the distribution for the
 368 sampler, and the best parameter and corresponding fitness value for each node is recorded; the best
 369 parameter is migrated across nodes every 50 generations. This procedure is repeated, until it reaches
 370 maximum generations.
 371

372 **Deployment environment** All the training were performed on 40 nodes, each containing 2 Intel®
 373 Xeon® Platinum 8358@2.60GHz CPU, and 512GB RAM, with 10 tasks per node.
 374

375 6 RESULTS

376 First, we benchmarked our BNN and a traditional SNN against the strong baseline performance
 377 achieved by MLP-PPO models reported in the literature. Schulman et al. (2017) Our intention is
 378 not to claim state-of-the-art results, but to evaluate the feasibility of evolutionary optimisation for
 379

Table 2: Performance of BNN-EAs, SNN-EAs, MLP-PPO, and MLP-TRPO approaches in the MuJoCo tasks trained for the same number of optimisation steps. For each task, the top 2 performances are highlighted in bold.

Methods	BNN-NES	BNN-CMA	SNN-NES	SNN-CMA	MLP-PPO	MLP-TRPO
Environment Steps	5×10^5					
Model(Size)	BNN(10,10)		SNN(10,10)		MLP(64,64)	
Task	Rewards					
CartPole	485.1 \pm 8.9	500\pm0	490.6 \pm 5.7	500\pm0	500\pm0	496.4 \pm 2.8
InvertedPendulum	863.7 \pm 40.3	1000.0\pm0.0	873.6 \pm 36.4	1000.0\pm0.0	217.8 \pm 99.6	842.3 \pm 33.9
InvertedDoublePendulum	203.5 \pm 11.5	348.3\pm13.4	127.1 \pm 5.9	289.1 \pm 22.0	4117.1\pm739.1	244.7 \pm 2.1
Swimmer	107.4 \pm 2.3	156.7 \pm 37.3	113.2 \pm 2.5	127.2 \pm 34.3	322.1\pm2.1	187.6\pm0.6
Ant	973.3\pm7.0	954.8\pm6.1	802.9 \pm 39.1	746.9 \pm 123.2	838.0 \pm 68.5	367.8 \pm 87.2
HalfCheetah	3187.4\pm36.8	2039.7 \pm 75.3	2265.2 \pm 25.9	1785.0 \pm 49.2	3818.6\pm120.3	2832.7 \pm 102.6
Hopper	2054.6\pm37.5	808.0 \pm 154.7	547.0 \pm 46.7	1190.2 \pm 40.3	780.3 \pm 174.7	2153.3\pm53.9
Walker2d	2261.1 \pm 90.6	1135.2 \pm 15.8	324.1 \pm 58.7	1044.4 \pm 5.2	1900.1 \pm 69.9	2427.9\pm105.3

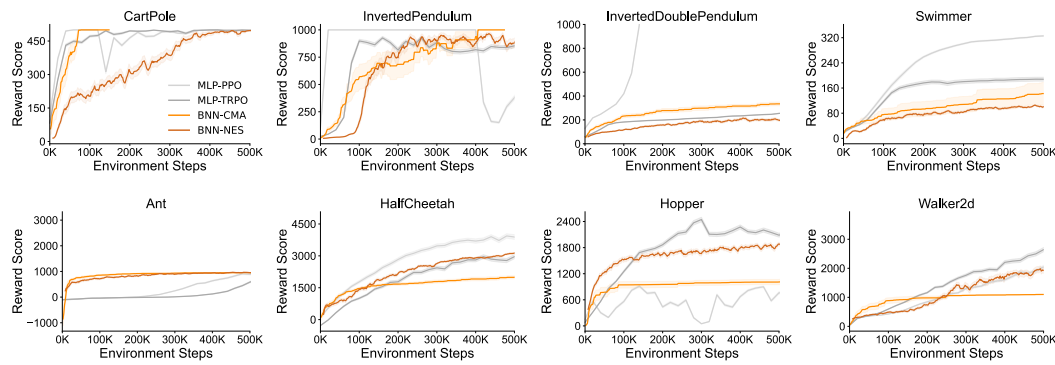


Figure 4: Training progress of BNN-CMA, BNN-NES, MLP-PPO and MLP-TRPO in 0.5 million steps.

biologically grounded networks. We trained BNN and SNN with two EAs, where the network size varied between 25 and 55 neurons, the most simple task CartPole requires 4 input neuron, 1 output neurons and 20 neurons in the E-I network, 25 neurons in total, and the most complicated task Ant requires 27 input neurons, 8 output neurons and 20 neurons in the E-I network, 55 neurons in total. The models were trained for up to 500 generations using both CMA-ES and NES, 1000 steps per generation. The results are illustrated in figure 3.

Results show that with substantially fewer training steps, our BNN achieves competitive performance for its parameter scale on most MuJoCo tasks. It consistently outperforms SNNs of the same scale and, on some tasks, achieves superior results with even fewer iterations. Furthermore, CMA-ES performs better on simpler tasks (top), whereas NES excels in more complex ones (bottom), consistent with the characteristics of their underlying energy landscapes (Figure 2B). This suggests the combination of the biological neurodynamic network and evolutionary algorithm (BNN-EA) is able to generate functional dynamic networks with effective task control capabilities in a much reduced model size, and with significantly fewer training steps.

To have a better insight into the training and convergence process, we further performed a comparison study between our BNN-EA approach, and SNN-EA, MLP gradient based approach. We trained a (64,64) MLP model with two hidden layers, with PPO and TRPO methods for the same 5×10^5 optimisation steps, and test them on MuJoCo control tasks. The results are summarised in table 2.

With the same number of optimisation steps, our BNN achieved comparable performance with MLP trained by PPO and TRPO. Furthermore, by inspecting the progression of the training, as illustrated in figure 4, suggests that our BNNs trained with EAs process similar learning dynamics as the mainstream reinforcement learning models and methods, and BNN-EAs has a higher sampling efficiency in the early stage of some complex tasks. Therefore the combination use of biological neurodynamic network and evolutionary algorithm training is a valid and feasible approach toward intelligence.

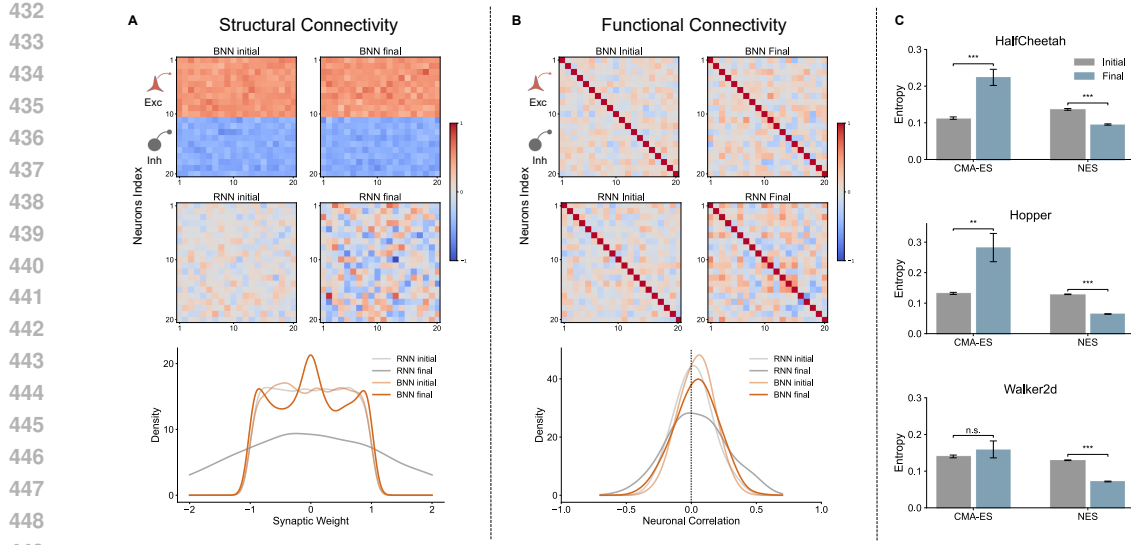


Figure 5: (A) The structural connection (SC) map of pre-trained and post-trained BNN (top) and RNN (middle). Colour describes the graded synapse, where red indicates excitatory, and blue indicates inhibitory. The distribution of the synapse weight is shown below. (B) The functional connection (FC) map of pre-trained and post-trained BNN (top) and RNN (middle). Colour describes the correlation, where red, and blue indicates one neuron has an excitatory, and inhibitory effect on the other neuron, respectively. The distribution of the neuron activity correlation is shown below. (C) The individual parameter distributions in BNN individuals of the CMA-ES and NES populations. ** $p<0.01$, *** $p<0.001$.

However, for environments such as InvertedDoublePendulum and Swimmer, the BNN demonstrates noticeably weaker performance than the MLP baseline. These tasks require rapid, high-frequency corrective control (InvertedDoublePendulum) or smooth, coordinated periodic actuation (Swimmer). Such behaviours are known to be more challenging for dynamical spiking-inspired models with fixed synaptic delays and continuous postsynaptic currents, especially without task-specific tuning. As a proof-of-principle study, our goal is not to reach peak performance on every environment, but to demonstrate that biologically realistic neural dynamics can be effectively optimized in continuous-control tasks.

To further investigate the network structure of the evolved biological neurodynamic networks, and to examine the capability of the evolutionary algorithm in terms of producing certain network structures during training, we analysed our BNN by calculating the correlation between neuronal firing and the synapse weights of the network, for the pre-trained and post-trained networks, on CartPole task. The pre-trained network is defined as the initial random network, and the network subjected to 100 generations of EA optimisation. For comparison, we also trained a recurrent neural network (RNN) of the same size, *i.e.*, 20 neurons, using the same EA setup and did the same analysis as for the BNN. The results are presented in figure 5.

First, we calculate the structural connection, *i.e.*, synapse weights that connect neurons in the network. Our results suggest that BNN develops certain structures during optimisation using the evolutionary algorithm. For BNN the synapse weights are evenly distributed between -1 and 1 initially, and gradually shift to either -1 or 1 after training, suggesting some excitatory and inhibitory connections are established during evolutionary optimisation, and the network evolves some certain structures in response to external environment, *i.e.*, control tasks. For comparison, the RNN model did not evolve into any structures, and the synapse weights are even more random than the initial state. This observation proves that our BNN is able to evolve a structured functional network via evolutionary optimisation. Similarly, we also analyse the functional correlation between the neurons, which describes whether one neuron has an excitatory (positively correlated) or inhibitory (negatively correlated) effect on the other neuron, thus providing insight into the internal dynamics of the network. The result suggests our BNN develops some correlations between neurons, as more

486 neuronal correlations are shifted away from zero, whereas the neuronal correlation distribution for
 487 RNN remains unchanged, suggesting no certain structures were formed during training for RNN.
 488

489 Figure 5C shows the parameter distribution of individuals within an EA population, measured by
 490 KL divergence, which served as an analogue to entropy in statistical thermodynamics. The parame-
 491 ter distribution provides an ideal indication of the parameter, or gene diversity of populations. Our
 492 results suggest that the CMA-ES algorithm tend to increase the parameter diversity, whereas for
 493 NES algorithm all individuals tend to converge to the same region in the parameter space. Popula-
 494 tions with better gene diversity are likely to preform well upon task switching, and therefore avoid
 495 catastrophic forgotten, thus presenting a promising pathway toward continual learning.
 496

497 7 DISCUSSION

498 The above described work shows that the combination use of our proposed biological neurody-
 499 namic networks and the evolutionary algorithms is capable of producing functional networks for
 500 control tasks with competitive performance given its significantly reduced model size, though not
 501 necessarily matching state-of-the-art gradient-based RL methods, and within a significantly fewer
 502 training steps. Furthermore, as a proof-of-principle study we demonstrate that the BNN can evolve
 503 certain network structures during evolution. Our BNN framework therefore provides a biologically
 504 grounded and interpretable route to intelligence, standing as a compelling parallel to mainstream
 505 reinforcement learning methodologies.

506 Beyond establishing performance feasibility, this framework enables controlled investigation of how
 507 biophysical mechanisms—such as synaptic delay heterogeneity, E–I population structure, and dy-
 508 namical stability—shape the emergence of functional behaviour in embodied tasks. Because these
 509 mechanisms are difficult to study using gradient-based methods and rarely appear jointly in prior
 510 evolutionary studies, our approach provides a testbed for quantifying the computational roles of
 511 biological dynamics in reinforcement-learning-like settings.

512 **513 Limitations and future works** Our current work focuses on small networks with only 20 neu-
 514 rons, whereas real biological brains typically contain millions or even billions of neurons. We al-
 515 ready achieved the state-of-the-art performance in most MuJoCo control tasks, and began to observe
 516 some certain network structures from evolution. Therefore we anticipate that by scaling up the BNN
 517 the control task performance will further increase, and more biologically relevant and interpretable
 518 structures will emerge, which would benefit both the neuroscience and reinforcement learning com-
 519 munity. Furthermore, the initial structure of our BNN is relatively simple, further development of
 520 the model can introduce extra layers or *a priori* empirical structures to improve the performance and
 521 bio-interpretability. In addition, the biologically realistic nature of BNN and EA allows us to fur-
 522 ther investigate the environment adaption behaviour of a population of individual networks using the
 523 analogue of thermodynamic entropy. Owing to the population based nature of EAs, we will in-
 524 vestigate the interplay between parameter (gene) diversity and task (environment) adaption capabilities
 525 in further studies.

526
 527
 528
 529
 530
 531
 532
 533
 534
 535
 536
 537
 538
 539

540 REFERENCES
541

542 Andrew G. Barto, Richard S. Sutton, and Charles W. Anderson. Neuronlike adaptive elements
543 that can solve difficult learning control problems. *IEEE Transactions on Systems, Man, and*
544 *Cybernetics*, SMC-13(5):834–846, September 1983. ISSN 2168-2909. doi: 10.1109/tsmc.1983.
545 6313077. URL <http://dx.doi.org/10.1109/TSMD.1983.6313077>.

546 Greg Brockman, Vicki Cheung, Ludwig Pettersson, Jonas Schneider, John Schulman, Jie Tang, and
547 Wojciech Zaremba. Openai gym, 2016. URL <https://arxiv.org/abs/1606.01540>.

548 Nicolas Brunel. Dynamics of sparsely connected networks of excitatory and inhibitory spiking
549 neurons. *Journal of Computational Neuroscience*, 8, 2000. ISSN 09295313. doi: 10.1023/A:
550 1008925309027.

552 T. F. Burns. Classic hebbian learning endows feed-forward networks with sufficient adaptability in
553 challenging reinforcement learning tasks. *Journal of Neurophysiology*, 125, 2021. ISSN 1522-
554 1598. doi: 10.1152/jn.00554.2020.

555 Sophie Denève and Christian K. Machens. Efficient codes and balanced networks, 2016. ISSN
556 15461726.

558 Sophie Denève, Alireza Alemi, and Ralph Bourdoukan. The brain as an efficient and robust adaptive
559 learner, 2017. ISSN 10974199.

561 Chris Eliasmith and Charles H Anderson. *Neural engineering: Computation, representation, and*
562 *dynamics in neurobiological systems*. MIT press, 2003.

563 Wulfram Gerstner, Werner M. Kistler, Richard Naud, and Liam Paninski. Neuronal Dynamics, jul
564 24 2014. URL <http://dx.doi.org/10.1017/CBO9781107447615>.

566 Marc-Oliver Gewaltig and Markus Diesmann. Nest (NEural Simulation Tool). *Scholarpedia*, 2(4):
567 1430, 2007. ISSN 1941-6016. doi: 10.4249/scholarpedia.1430. URL <http://dx.doi.org/10.4249/scholarpedia.1430>.

569 K. G. Habashy, B. D. Evans, D. F. Goodman, and J. S. Bowers. Adapting to time: Why nature may
570 have evolved a diverse set of neurons. *PLOS Computational Biology*, 20(12):e1012673, 2024.
571 doi: 10.1371/journal.pcbi.1012673.

573 Bilal Haider and David A. McCormick. Rapid neocortical dynamics: Cellular and network mecha-
574 nisms, 2009. ISSN 08966273.

575 Nikolaus Hansen, Sibylle D Müller, and Petros Koumoutsakos. Reducing the time complexity of
576 the derandomized evolution strategy with covariance matrix adaptation (cma-es). *Evolutionary*
577 *computation*, 11(1):1–18, 2003.

579 Guillaume Hennequin, Tim P. Vogels, and Wulfram Gerstner. Optimal control of transient dynamics
580 in balanced networks supports generation of complex movements. *Neuron*, 82, 2014. ISSN
581 10974199. doi: 10.1016/j.neuron.2014.04.045.

582 Sepp Hochreiter and Jürgen Schmidhuber. Long short-term memory. *Neural Computation*, 9(8):
583 1735–1780, November 1997. ISSN 1530-888X. doi: 10.1162/neco.1997.9.8.1735. URL <http://dx.doi.org/10.1162/neco.1997.9.8.1735>.

586 A L Hodgkin and A F Huxley. A quantitative description of ion currents and its applications to
587 conduction and excitation in nerve membranes. *Journal of Physiology*, 117, 1952.

588 Kurt Hornik, Maxwell Stinchcombe, and Halbert White. Multilayer feedforward networks are uni-
589 versal approximators. *Neural Networks*, 2(5):359–366, January 1989. ISSN 0893-6080. doi: 10.
590 1016/0893-6080(89)90020-8. URL [http://dx.doi.org/10.1016/0893-6080\(89\)90020-8](http://dx.doi.org/10.1016/0893-6080(89)90020-8).

593 Alessandro Ingrosso and L. F. Abbott. Training dynamically balanced excitatory-inhibitory net-
594 works. *PLoS ONE*, 14, 2019. ISSN 19326203. doi: 10.1371/journal.pone.0220547.

594 Jeffry S. Isaacson and Massimo Scanziani. How inhibition shapes cortical activity, 2011. ISSN
 595 08966273.

596

597 E. M. Izhikevich. Polychronization: Computation with spikes. *Neural Computation*, 18(2):245–282,
 598 2006. doi: 10.1162/089976606775093882.

599

600 Yann LeCun, Geoffrey Hinton, and Yoshua Bengio. Deep learning (2015), y. lecun, y. bengio and
 601 g. hinton. *Nature*, 521, 2015.

602 Gehua Ma, Rui Yan, and Huajin Tang. Exploiting noise as a resource for computation and learning
 603 in spiking neural networks. *Patterns*, 4(10):100831, 10 2023. ISSN 2666-3899. doi: 10.1016/j.patter.
 604 2023.100831. URL <http://dx.doi.org/10.1016/j.patter.2023.100831>.

605

606 Wolfgang Maass. Networks of spiking neurons: The third generation of neural network models.
 607 *Neural Networks*, 10, 1997. ISSN 08936080. doi: 10.1016/S0893-6080(97)00011-7.

608

609 Wolfgang Maass and Henry Markram. On the computational power of circuits of spiking neurons.
 610 *Journal of Computer and System Sciences*, 69, 2004. ISSN 00220000. doi: 10.1016/j.jcss.2004.
 611 04.001.

612

613 H. Markram, W. Gerstner, and P. J. Sjöström. Spike-timing-dependent plasticity: A comprehensive
 614 overview, 2012. ISSN 16633563.

615

616 Warren S. McCulloch and Walter Pitts. A logical calculus of the ideas immanent in nervous activity.
 617 *The Bulletin of Mathematical Biophysics*, 5, 1943. ISSN 00074985. doi: 10.1007/BF02478259.

618

619 Balázs Mészáros, James C. Knight, and Thomas Nowotny. Learning delays through gradients and
 620 structure: emergence of spatiotemporal patterns in spiking neural networks. *Frontiers in Computational
 621 Neuroscience*, 18, dec 20 2024. ISSN 1662-5188. doi: 10.3389/fncom.2024.1460309.
 622 URL <http://dx.doi.org/10.3389/fncom.2024.1460309>.

623

624 Volodymyr Mnih, Koray Kavukcuoglu, David Silver, Andrei A. Rusu, Joel Veness, Marc G. Bellemare,
 625 Alex Graves, Martin Riedmiller, Andreas K. Fidjeland, Georg Ostrovski, Stig Petersen,
 626 Charles Beattie, Amir Sadik, Ioannis Antonoglou, Helen King, Dharshan Kumaran, Daan Wierstra,
 627 Shane Legg, and Demis Hassabis. Human-level control through deep reinforcement learning.
 628 *Nature*, 518, 2015. ISSN 14764687. doi: 10.1038/nature14236.

629

630 Milad Mozafari, Mohammad Ganjtabesh, Abbas Nowzari-Dalini, Simon J. Thorpe, and Timothée
 631 Masquelier. Bio-inspired digit recognition using reward-modulated spike-timing-dependent plasticity
 632 in deep convolutional networks. *Pattern Recognition*, 94, 2019. ISSN 00313203. doi:
 633 10.1016/j.patcog.2019.05.015.

634

635 E. Najarro and S. Risi. Meta-learning through hebbian plasticity in random networks. In *Advances
 636 in Neural Information Processing Systems*, volume 33, pp. 20719–20731, 2020.

637

638 Emre O. Neftci, Hesham Mostafa, and Friedemann Zenke. Surrogate gradient learning in spiking
 639 neural networks: Bringing the power of gradient-based optimization to spiking neural networks.
 640 *IEEE Signal Processing Magazine*, 36, 2019. ISSN 15580792. doi: 10.1109/MSP.2019.2931595.

641

642 Allen Newell, J. C. Shaw, and Herbert A. Simon. Elements of a theory of human problem solving.
 643 *Psychological Review*, 65, 1958. ISSN 0033295X. doi: 10.1037/h0048495.

644

645 Tobias C. Potjans and Markus Diesmann. The cell-type specific cortical microcircuit: Relating
 646 structure and activity in a full-scale spiking network model. *Cerebral Cortex*, 24, 2014. ISSN
 647 10473211. doi: 10.1093/cercor/bhs358.

648

649 Peng Qu, Hui Lin, Meng Pang, Xiaofei Liu, Weimin Zheng, and Youhui Zhang. Enlarge: An effi-
 650 cient snn simulation framework on gpu clusters. *IEEE Transactions on Parallel and Distributed
 651 Systems*, 34, 2023. ISSN 15582183. doi: 10.1109/TPDS.2023.3291825.

652

653 F. Rosenblatt. The perceptron: A probabilistic model for information storage and organization in
 654 the brain. *Psychological Review*, 65, 1958. ISSN 0033295X. doi: 10.1037/h0042519.

648 David E. Rumelhart, Geoffrey E. Hinton, and Ronald J. Williams. Learning representations by
 649 back-propagating errors. *Nature*, 323(6088):533–536, October 1986. ISSN 1476-4687. doi:
 650 10.1038/323533a0. URL <http://dx.doi.org/10.1038/323533a0>.

651

652 Tim Salimans, Jonathan Ho, Xi Chen, Szymon Sidor, and Ilya Sutskever. Evolution strategies as
 653 a scalable alternative to reinforcement learning, 2017a. URL <https://arxiv.org/abs/1703.03864>.

654

655 Tim Salimans, Jonathan Ho, Xi Chen, Szymon Sidor, and Ilya Sutskever. Evolution strategies as
 656 a scalable alternative to reinforcement learning, 2017b. URL <https://arxiv.org/abs/1703.03864>.

657

658 Jeffrey R Sampson. Adaptation in natural and artificial systems (john h. holland), 1976.

659

660 Maximilian Schmidt, Rembrandt Bakker, Kelly Shen, Gleb Bezgin, Markus Diesmann, and
 661 Sacha Jennifer van Albada. A multi-scale layer-resolved spiking network model of resting-
 662 state dynamics in macaque visual cortical areas. *PLoS Computational Biology*, 14, 2018. ISSN
 663 15537358. doi: 10.1371/journal.pcbi.1006359.

664

665 John Schulman, Sergey Levine, Pieter Abbeel, Michael Jordan, and Philipp Moritz. Trust region
 666 policy optimization. In Francis Bach and David Blei (eds.), *Proceedings of the 32nd International
 667 Conference on Machine Learning*, volume 37 of *Proceedings of Machine Learning Research*, pp.
 668 1889–1897, Lille, France, 07–09 Jul 2015. PMLR. URL <https://proceedings.mlr.press/v37/schulman15.html>.

669

670 John Schulman, Filip Wolski, Prafulla Dhariwal, Alec Radford, and Oleg Klimov. Proximal policy
 671 optimization algorithms, 2017. URL <https://arxiv.org/abs/1707.06347>.

672

673 Michael N. Shadlen and William T. Newsome. Noise, neural codes and cortical organiza-
 674 tion. *Current Opinion in Neurobiology*, 4(4):569–579, 8 1994. ISSN 0959-4388. doi: 10.
 675 1016/0959-4388(94)90059-0. URL [http://dx.doi.org/10.1016/0959-4388\(94\)90059-0](http://dx.doi.org/10.1016/0959-4388(94)90059-0).

676

677 G. Shen, D. Zhao, Y. Dong, and Y. Zeng. Brain-inspired neural circuit evolution for spiking neural
 678 networks. *Proceedings of the National Academy of Sciences*, 120(39):e2218173120, 2023. doi:
 679 10.1073/pnas.2218173120.

680

681 H. Francis Song, Guangyu R. Yang, and Xiao Jing Wang. Training excitatory-inhibitory recurrent
 682 neural networks for cognitive tasks: A simple and flexible framework. *PLoS Computational
 683 Biology*, 12, 2016. ISSN 15537358. doi: 10.1371/journal.pcbi.1004792.

684

685 Kenneth O. Stanley and Risto Miikkulainen. Evolving neural networks through augmenting topolo-
 686 gies. *Evolutionary Computation*, 10, 2002. ISSN 10636560. doi: 10.1162/106365602320169811.

687

688 Kenneth O Stanley, David B D’Ambrosio, and Jason Gauci. A hypercube-based encoding for evolv-
 689 ing large-scale neural networks. *Artificial life*, 15(2):185–212, 2009.

690

691 Piergiorgio Strata and Robin Harvey. Dale’s principle. *Brain Research Bulletin*, 50(5–6):349–350,
 692 November 1999. ISSN 0361-9230. doi: 10.1016/s0361-9230(99)00100-8. URL [http://dx.doi.org/10.1016/S0361-9230\(99\)00100-8](http://dx.doi.org/10.1016/S0361-9230(99)00100-8).

693

694 Felipe Petroski Such, Vashisht Madhavan, Edoardo Conti, Joel Lehman, Kenneth O. Stanley, and
 695 Jeff Clune. Deep neuroevolution: Genetic algorithms are a competitive alternative for training
 696 deep neural networks for reinforcement learning, 2018. URL <https://arxiv.org/abs/1712.06567>.

697

698 Emanuel Todorov, Tom Erez, and Yuval Tassa. Mujoco: A physics engine for model-based control.
 699 In *IEEE International Conference on Intelligent Robots and Systems*, 2012. doi: 10.1109/IROS.
 700 2012.6386109.

701 C. Van Vreeswijk and H. Sompolinsky. Chaos in neuronal networks with balanced excitatory and
 702 inhibitory activity. *Science*, 274, 1996. ISSN 00368075. doi: 10.1126/science.274.5293.1724.

702 X.-J. Wang. Synaptic basis of cortical persistent activity: the importance of nmda receptors to
703 working memory. *Journal of Neuroscience*, 19(21):9587–9603, 1999.
704

705 Daan Wierstra, Tom Schaul, Tobias Glasmachers, Yi Sun, Jan Peters, and Jürgen Schmidhuber.
706 Natural evolution strategies. *Journal of Machine Learning Research*, 15, 2014. ISSN 15337928.
707

708 Jeffery A. Winer. Anatomy of the cortex: Statistics and geometry. v. braitenberg , a. schuz. *The*
709 *Quarterly Review of Biology*, 68, 1993. ISSN 0033-5770. doi: 10.1086/418002.
710

711 Kong Fatt Wong and Xiao Jing Wang. A recurrent network mechanism of time integration in percep-
712 tual decisions. *Journal of Neuroscience*, 26, 2006. ISSN 02706474. doi: 10.1523/JNEUROSCI.
713 3733-05.2006.

714 Esin Yavuz, James Turner, and Thomas Nowotny. Genn: A code generation framework for acceler-
715 ated brain simulations. *Scientific Reports*, 6, 2016. ISSN 20452322. doi: 10.1038/srep18854.
716

717 Anthony M. Zador. A critique of pure learning and what artificial neural networks can learn from
718 animal brains, 2019. ISSN 20411723.
719
720
721
722
723
724
725
726
727
728
729
730
731
732
733
734
735
736
737
738
739
740
741
742
743
744
745
746
747
748
749
750
751
752
753
754
755

756 Appendix

759 A BIOLOGICAL NEURODYNAMIC MODELS

761 **Model for neuron** Neurodynamic models require neuron models to describe the dynamics of neurons, *i.e.*, signal firing. Multiple models for neurons have been proposed; among them, the Leaky 762 Integrate-and-Fire (LIF) neuron Gerstner et al. (2014) has been proved to be a biologically realistic 763 and computationally feasible one. The state of LIF neurons can be expressed as:

$$766 \quad C_m \frac{dv(t)}{dt} = -\frac{C_m}{\tau_m} [v(t) - v(\text{rest})] + i_e(t) + i_i(t) + I_{\text{offset}} + I_{\text{injection}}(t), \quad (1)$$

$$769 \quad \text{if } V(t) > V_{\text{th}}, V_t \leftarrow V_{\text{reset}}, \quad (2)$$

770 where C_m is the neuron capacity, $v(t)$ is the membrane voltage, τ_m is the membrane time constant, $v(\text{rest})$ is the resistant voltage, $i_e(t)$ and $i_i(t)$ are the excitatory and inhibitory input currents, 771 respectively, and I_{offset} and $I_{\text{injection}}(t)$ are the constant / noisy input currents. If the membrane 772 voltage $v(t)$ reaches the threshold V_{th} , the neuron will issue a signal, and $v(t)$ will be held at $v(\text{rest})$ 773 for a refractory period τ_{ref} . Once this refractory period ends, the neuron follows this expression until 774 it issues the next signal again.

775 **Model for synapse** In addition to neurons, the connections between them, *i.e.*, synapses, are crucial 776 in biological neural networks. Gerstner et al. (2014) Synapses transmit electrical signals from 777 presynaptic to postsynaptic neurons, it defines how signals fired by neurons affect the membrane 778 voltage of a postsynaptic neuron. In the model for synapses, it has the impulse signal in presynaptic 779 neurons as the input, and the postsynaptic current as the output. The postsynaptic current (PSC) can 780 be expressed as:

$$784 \quad I_{\text{syn}} = g(t)(V_{\text{post}} - E_{\text{syn}}), \quad (3)$$

785 where I_{syn} is the postsynaptic current, V_{post} is the postsynaptic voltage, E_{syn} is the reversal potential 786 of the synapse; its value determines whether a synapse is either excitatory or inhibitory, and g is the 787 conductance on synapses.

788 In phenomenological models, *i.e.*, synapse is modelled based on the postsynaptic current, rather than 789 the dynamical features of the ion channels, the time-dependence of $g(t)$ can be expressed as:

$$793 \quad g_t = \bar{g} \sum_{t^{(f)}} s(t - t^{(f)}), \quad (4)$$

794 where \bar{g} is a constant describing the synapse weight, $t^{(f)}$ denotes the moment that the signal arrives 795 at the synapse, $s(t - t^{(f)})$ is a time-dependent function that describes the effect of signal firing on 796 g_t . Using an exponential decay to model the synapses, we obtain:

$$801 \quad s(t) = e^{-t/\tau} H(t), \quad (5)$$

802 where τ is a temporal constant, and $H(t)$ is the heaviside function. We introduce synaptic delay as a 803 new parameter for better biological interoperability, the $g(t)$ differential equation of g_t , with respect 804 to the current time is therefore:

$$808 \quad \frac{dg}{dt} = -\frac{g}{\tau} + \bar{g} \sum_{t^{(f)}, k} \delta(t - t^{(f)} - d^k). \quad (6)$$

810 Where δ function is zero anywhere but $t = 0$, and t is the current time, d^k is the transmission delay
 811 corresponding to the k^{th} synapse.

812 Unlike most ANN and SNN benchmarks that assume uniform synaptic delays, biological synapses
 813 exhibit heterogeneous conduction and transmission latencies. Such delay variability has been
 814 shown to create rich temporal structures—including polychronous firing assemblies (Izhikevich
 815 (2006))—which increase memory capacity and extend the temporal credit-assignment horizon. Opti-
 816 mising delays therefore expands the dynamical repertoire of the BNN beyond what can be achieved
 817 using weights alone.

818 The parameters for neuron and synapse models employed in the work described in this paper are
 819 summarised in table 3.

822 Table 3: Parameters for the Biological Neurodynamic Model.

Parameter	Value	Unit
Resting potential (V_{rest})	-60	mV
Reset potential (V_{reset})	-60	mV
Initial membrane potential (V_0)	-55	mV
Threshold potential (V_{th})	-50	mV
Membrane capacitance (C_m)	1	pF
Membrane time constant (τ_m)	20	ms
Synaptic time constant (τ_{syn})	5	ms

B BIOLOGICAL NEURODYNAMIC NETWORKS

832 **Excitatory–Inhibitory Balance Models** Excitatory–inhibitory (E–I) balance Vreeswijk & Som-
 833 polinsky (1996) is a hallmark of cortical microcircuitry, whereby excitatory and inhibitory synaptic
 834 inputs dynamically counterbalance each other to maintain stable yet flexible neural activity. This
 835 principle, rooted in electrophysiological recordings from the neocortex and hippocampus, has in-
 836 spired a class of computational models that preserve this balance at both the single-neuron and
 837 population level. These E–I balanced networks typically consist of spiking neurons or rate-based
 838 models partitioned into excitatory and inhibitory subpopulations, with constrained synaptic weights
 839 (e.g., Dale’s law Strata & Harvey (1999)) and recurrent connectivity that gives rise to asynchronous
 840 irregular activity, criticality, and efficient coding. The E–I architecture has been shown to support
 841 robust computations, including working memory, pattern decorrelation, and gain control, by lever-
 842 aging biologically plausible dynamics rather than task-specific training. Notably, such models often
 843 operate without supervised gradient-based optimization, instead relying on biologically motivated
 844 plasticity rules or structured connectivity to enable function.

845 The parameters for the biological neurodynamic network (BNN) employed in the work described in
 846 this paper are summarised in table 4.

850 Table 4: Parameters for the Biological Neurodynamic Model.

Parameter	Value	Unit
Simulation duration	100	timestep
Simulation step size	0.1	ms
Number of neurons	10E + 10I + number of input&output	-
Learnable Params	synaptic weights and delays, noisy input	-

C SPIKING NEURAL NETWORKS

856 Spiking neural networks (SNNs) Maass (1997); Maass & Markram (2004) emulate the dynamics
 857 of real neurons by encoding and transmitting information via discrete spikes. Neurons in SNNs
 858 integrate synaptic inputs over time and emit spikes when membrane potentials exceed threshold,
 859 introducing an inherent temporal dimension and nonlinearity that makes them both biologically
 860 plausible and computationally distinct. Unlike MLPs, where activations are continuously differen-
 861 tiable, SNNs rely on non-differentiable events, posing challenges for standard optimization methods

864 and prompting the development of surrogate gradients, spike-based learning rules, and biologically
 865 inspired plasticity mechanisms. Furthermore, the asynchronous and sparse firing nature of SNNs
 866 facilitates event-driven computation, offering potential gains in energy efficiency when deployed on
 867 neuromorphic hardware. Thus, while MLPs excel in data-rich, high-throughput regimes with dense
 868 numerical representations, SNNs offer a promising alternative for real-time, low-power, and biolog-
 869 ically grounded computation, particularly in scenarios demanding temporal precision and structural
 870 interpretability.

871

872 D ARTIFICIAL NEURAL NETWORKS

873

874 Alongside our proposed biological neurodynamic networks (BNNs), the following artifical neural
 875 networks LeCun et al. (2015) are considered in the work described in this papar.

876

877 **Multilayer perceptrons** Multilayer perceptrons (MLPs) Hornik et al. (1989) are feedforward neu-
 878 ral networks that compute deterministic, continuous-valued transformations through stacked layers
 879 of weighted summations and pointwise nonlinearities. As universal function approximators, MLPs
 880 form the backbone of modern deep learning, enabling supervised and unsupervised learning across
 881 vision, language, and control domains. Their success is rooted in architectural simplicity, differ-
 882 entiability, and compatibility with efficient gradient-based training methods such as backpropaga-
 883 tion. However, MLPs operate in discrete time with synchronous updates and dense, analog acti-
 884 vations—features that stand in sharp contrast to the event-driven, temporally sparse computations
 885 observed in biological neural circuits.

886

887 **Recurrent Neural Networks** Recurrent neural networks (RNNs) Rumelhart et al. (1986) are a
 888 foundational class of artificial neural models developed to handle sequential and temporally struc-
 889 tured data. Unlike feedforward architectures, RNNs maintain internal state through recurrent con-
 890 nections, allowing them to capture dynamic dependencies across time. Variants such as Long Short-
 891 Term Memory (LSTM) Hochreiter & Schmidhuber (1997) networks and Gated Recurrent Units
 892 (GRUs) were introduced to overcome vanishing gradient issues and have since become standard
 893 tools in natural language processing, time series forecasting, and reinforcement learning. While
 894 RNNs exhibit impressive performance in engineering tasks, they lack constraints from biological
 895 connectivity and synaptic dynamics. Their recurrent activity arises from parameterized weight ma-
 896 trices and nonlinear activations, rather than the structured E–I coupling observed in cortical net-
 897 works. As such, RNNs prioritize trainability and function approximation over mechanistic inter-
 898 pretability. Efforts to bridge this gap have emerged through hybrid models, such as balanced RNNs
 899 or spiking RNNs with biologically inspired constraints, but a fundamental divergence remains: E–I
 900 balance models are grounded in the physical dynamics of neural tissue, while RNNs abstract away
 901 biological detail to maximize learning flexibility.

902

903 The key differences between MLP, SNN and our BNN are summarised in table 5.

904

905

906 **Table 5: Comparison of different network architectures.**

907 Network Architecture	908 Artificial Neural Network	909 Spiking Neural Network	910 Biological Neurodynamic Network
911 Basic Unit	Weighted sum + nonlinear activation	integrate-and-fire	LIF + Synaptic dynamics
912 Neural Dynamics	Static	Temporal integration	Membrane potential + conductance dynamics
913 Information Encoding	Continuous values	Spike trains	Continuous dynamical state
914 Computational Efficiency	High (GPU friendly)	Medium (requires event-driven framework)	Low to Medium (complex simulation)
915 Application Domain	Image recognition, NLP	Brain-inspired computation	Brain modeling, biophysical simulations

916

917

918 E PARALLEL SIMULATION FRAMEWORK

919

920 The parallel neurodynamics simulation framework ENLARGE Qu et al. (2023) is employed. We
 921 mainly use the fine-grained network representation and hierarchical communication architecture in
 922 ENLARGE.

923

924

925 Fine-grained impulse neural network represents and stores neuron and synapse parameters, and net-
 926 work topology separately. The neuron and synapse parameters are firstly separated and grouped
 927 according to the characteristics of the computational units and distributed memory. The commu-
 928 nication paths are then optimised by the segmentation algorithm to reduce the redundant commu-

918 nication between clusters. Compressed sparse row (CSR) analogy is used for network topology
 919 information to describe the connection information of each individual neurons and synapses. For
 920 the fine-grained pulsed neural network representation, the delay information is integrated into the
 921 CSR representation to form a compact network representation, which dramatically saves the storage
 922 requirement.

923 The hierarchical communication architecture divides cluster communication into three levels: pro-
 924 cess level, intra-node level and inter-node level. It provides two main modules: the converter module
 925 and the communication module. The former locates in the process, which queries the firing neuron
 926 ID from the firing list, and converts it into the corresponding shadow neuron ID; it also rearranges
 927 the shadow neuron IDs according to their destinations. The latter handles most of the communica-
 928 tion and synchronisation. All core computations are performed in the process, the firing list is stored
 929 and accessed at each computation phases for data sharing. The synchronisation occurs only at the
 930 inter-node level. As the global time must be synchronised within each time step, the hierarchical
 931 communication architecture transmits the data in a blocking manner in order to reduce the cost. This
 932 blocking communication process can also be used as a synchronisation signal, instead of the actual
 933 synchronisation process of the global time.

934 935 F PARALLEL EVOLUTIONARY ALGORITHM

936 We considered two implementations of the evolutionary algorithms, CMA-ES Hansen et al. (2003)
 937 and NES Wierstra et al. (2014). The pusedocode is presented in **Algorithm F** and **Algorithm F**.

938 Parallel CMA-ES Algorithm **Input:** Initial network parameters θ_0 , noise standard deviation σ .
 939 **Output:** Optimal network weights W .

940 **Initialise:** m nodes, n tasks.

941 generation < generation limit each nodes i=1 to m each tasks j=1 to n Generate a polpulation of
 942 network parameters using CMA-ES sampler;

943 Parallel compute fitness score F_j and return to CMA-ES;

944 Update CMA-ES sampler's distribution;

945 Record best parameter σ_i , best score F_i of all tasks;

946 generation = migrate generation Exchange best parameter θ_i , best score F_i to every other nodes;
 947 Save network weights with highest score W_{best} .

948 Parallel NES Algorithm **Input:** Initial network parameters θ_0 , noise standard deviation σ .

949 **Output:** Optimal network weights W .

950 **Initialise:** m nodes, n tasks.

951 generation < generation limit each nodes i=1 to m each tasks j=1 to n Generate a polpulation of
 952 network parameters using NES sampler;

953 Parallel compute fitness score F_j and return to NES;

954 Update NES sampler's distribution;

955 Record best parameter σ_i , best score F_i of all tasks;

956 generation = migrate generation Exchange best parameter θ_i , best score F_i to every other nodes;
 957 Save network weights with highest score W_{best} .

958 The parameters for evolutionary algorithms employed in the work presented in this paper are listed
 959 in table 6.

960 961 962 963 964 965 Table 6: Parameters of Evolutionary Algorithm.

966 Parameter	967 Value
968 Population size (λ)	10
969 Parent size (μ)	$\lambda/2$
970 Initial step size (σ)	0.5
Initial mean	Uniform($[0, 1]^n$)
Max generation	500

972 **G REINFORCEMENT LEARNING TRAINING ALGORITHMS**
973974 We consider two RL training techniques, PPO Schulman et al. (2017) and TRPO Schulman et al.
975 (2015) in the current work. The parameters during network training presented in the work described
976 in this paper are listed in table 7.
977978 **Table 7: PPO and TRPO parameters used for Mujoco tasks.**
979

980 Parameter	981 Value	982 Description
983 Policy Net	984 MLP	985 2 layers with 64 units each
986 Learning rate	987 3×10^{-4}	988 Adam optimizer
989 Discount factor (γ)	990 0.99	991 Reward discounting
992 GAE lambda (λ)	993 0.95	994 For Generalized Advantage Estimation
995 Batch size	996 64	997 Mini-batch size for updates
998 Rollout length	999 2048	1000 Timesteps per batch
1001 Epochs per update	1002 10	1003 Number of gradient steps per batch

1004 **H EXPERIMENTS**
10051006 **CartPole** CartPole Barto et al. (1983) is a 2-dimensional control task in which the intelligent agent
1007 needs to keep a pole balanced upright by applying discrete left and right thrusts. The task, which
1008 is widely regarded as a standard test for assessing the responsiveness and stability of a controller.
1009 The state space is four-dimensional, comprising the cart’s position and velocity, as well as the pole’s
1010 angle and angular velocity. The 2-dimensional action space consists of two discrete actions repre-
1011 senting forces applied to the left or right. The reward of the intelligent agent is determined by the
1012 positive feedback gained from successfully maintaining the equilibrium state at each time step, and
1013 the task continues until the pole tilt angle or position exceeds a threshold value.
10141015 **MuJuCo Tasks** The MuJoCo tasks Todorov et al. (2012) we chose are mainly robot motion
1016 control problems with a high-dimensional state space (8-27 dimensions) and a continuous action space
1017 (1-8 dimensions), where the state contains information about the position, velocity, angle, and an-
1018 gular velocity of the body parts, and the action represents the control signals applied to the actuated
1019 joints. The reward functions primarily based on the the distance travelled along a specific axis,
1020 complemented by an energy penalty term and balance constraints. Each task is set as a finite time
1021 trajectory of 1000 steps.
1022